



SAKARYA ÜNİVERSİTESİ

FEN BİLİMLERİ ENSTİTÜSÜ DERGİSİ

Sakarya University Journal of Science
SAUJS

e-ISSN 2147-835X | Period Bimonthly | Founded: 1997 | Publisher Sakarya University |
<http://www.saujs.sakarya.edu.tr/en/>

Title: Microstructures and Phase Transformations of Melt-Spun Ti-V-Al high Temperature Shape Memory Alloys with Addition of Zr

Authors: Öznur BAĞ, Fikret YILMAZ, Uğur KÖLEMEN, Semra ERGEN

Received: 2020-09-21 16:21:45

Accepted: 2021-04-23 11:17:32

Article Type: Research Article

Volume: 25

Issue: 3

Month: June

Year: 2021

Pages: 735-740

How to cite

Öznur BAĞ, Fikret YILMAZ, Uğur KÖLEMEN, Semra ERGEN; (2021), Microstructures and Phase Transformations of Melt-Spun Ti-V-Al high Temperature Shape Memory Alloys with Addition of Zr. Sakarya University Journal of Science, 25(3), 735-740, DOI:

<https://doi.org/10.16984/saufenbilder.797337>

Access link

<http://www.saujs.sakarya.edu.tr/en/pub/issue/62736/797337>

New submission to SAUJS

<http://dergipark.org.tr/en/journal/1115/submission/step/manuscript/new>

Microstructures and Phase Transformations of Melt-Spun Ti-V-Al high Temperature Shape Memory Alloys with Addition of Zr

Öznur BAĞ*¹, Fikret YILMAZ¹, Uğur KÖLEMEN², Semra ERGEN¹

Abstract

In this study, the effects of Zr addition on phase transformation temperatures, microstructure of Ti-12V-4Al (wt. %) high temperature shape memory alloys (HTSMAs) manufactured using melt-spinning technique were investigated. During heating, differential scanning calorimetry (DSC) curves showed that austenite transformation temperature of Ti-12V-4Al (wt. %) melt-spun ribbon was single-stage transformation and Ti-12V-4Al-0.5Zr (wt. %) melt-spun ribbon was two-stage transformation. In the scanning electron microscopy (SEM) and X-ray diffraction (XRD) analyzes, unveiled that the melt-spun ribbons consisted of martensite, austenite and R phases. Transmission electron microscopy (TEM) analysis showed that the thickness of martensite plates in ribbons was thinned by the addition of Zr.

Keywords: High temperature, shape memory alloys, phase transition

1. INTRODUCTION

Shape memory alloys (SMAs) can recover their deformed shape are smart materials. The driving forces of this reversible deformation are; there may be load, temperature and magnetic effect. The reason for this feature, which is not seen in traditional metals and alloys, is the solid-solid phase transformations, which are defined as thermo-elastic martensitic phase transformation [1]. Thanks to these reversible phase transformations, shape memory alloys can regain their original state after being deformed. Furthermore, shape memory alloys show superelastic properties and are highly they can remain elastic under stresses. Shape memory

alloys are materials that can be used in many fields such as vibration damping, noise reduction, sensors, building, biomedical due to their shape memory and superelasticity properties. NiTi alloys come into prominence due to their good functional and mechanical properties such as ductility, fatigue strength and deformation rate. However, as the transformation temperatures of NiTi alloys are below 100 °C, high temperatures such as aerospace, automobile and oil industry its use is limited in areas that require [2]. Therefore, researchers are working to develop materials with transformation temperatures above 100 °C.

As a result of the researches, many high temperature shape memory alloys have been

*Corresponding author: oznurbag@gmail.com

¹Gaziosmanpaşa University, Faculty of Arts and Science, Department of Physics, 60240, Tokat.

E-mail: oznurbag@gmail.com; fikreyilmaz79@gmail.com; semraergengop@gmail.com

ORCID: <https://orcid.org/0000-0002-9944-8221>; <https://orcid.org/0000-0002-1835-4961>; <https://orcid.org/0000-0002-5515-0933>

²Yozgat Bozok University, Faculty of Arts and Science, Department of Physics, 66100, Yozgat.

E-mail: ugur.kolemen@bozok.edu.tr

ORCID: <https://orcid.org/0000-0001-9858-8823>

found by adding the third element to the binary alloys.

Ti-based alloys are one of the best examples for high temperature shape memory alloys (HTSMAs). Ti-V-Al alloys, which are Ti-based alloys, have low density and have high heat resistance, strength, flexibility, toughness, processability, weldability, corrosion resistance and biocompatibility. Therefore, it is advantageous for use in many high temperature applications, especially in aviation applications. Among the alloying elements added to titanium, the most well-known elements such as Al, Sn, Ga and Zr perform well at high temperatures.

The Zr element, which is generally considered to be a neutral element and compatible with the Ti group, is often added to improve mechanical and shape memory properties [3, 4, 5, 6].

Melt-spinning is the most adopted technique among rapid solidification techniques owing to its high cooling rate (10^5 – 10^7 °C/s) and simple application. This technique is typically used to create thin metal or alloy ribbons of a certain atomic structure. The melt spinning technique produces a fine-grained microstructure, increasing the solubility of alloying elements and reducing levels of dissociation [7, 8]. These effects can lead to advancements in shape memory alloy systems in terms of shape memory capabilities and superelasticity [9].

In this study, Zr was added to Ti-12V-4Al (wt. %) alloy for the first time and Ti-12V-4Al-0.5Zr (wt. %) ribbon alloy was produced by melt spinning technique. The aim of this work is to investigate the effect of Zr addition on the microstructural evolution and phase transformation temperature of Ti-12V-4Al (wt. %) high temperature shape memory alloy. The microstructure, phase formation, chemical composition and transformation temperatures were examined by using differential scanning calorimetry (DSC), X-ray diffraction (XRD), optic microscope (OM), scanning electron microscopy (SEM) and transmission electron microscopy (TEM).

2. MATERIAL AND METHODS

Firstly, elemental Ti (99.9 % purity), V (99.999 % purity), Al (99.9 %) and Zr (99.9 %) were used to prepare the alloy of nominal composition Ti-12V-4Al and Ti-12V-4Al-0.5Zr. In this study, all percentages are wt. % unless otherwise stated. The alloys were first melted under an argon atmosphere by an arc-melter system. In order to ensure homogenization, the alloys were repeatedly melted three times and then annealed at a temperature of 950 °C for 6 h in vacuum-sealed quartz crucibles. And then was quenched in ice water by breaking the crucible. Afterward, the master alloys were cut into small pieces for rapid solidification by melt-spinning. Then rapidly solidified counter part of the master alloys were prepared using an Edmund Buhler SC melt-spinner. For the melt-spinning process, Ti-12V-4Al (wt. %) and Ti-12V-4Al-0.5Zr (wt. %) master alloys with a weight of about 3 g were prepared and the alloys were placed in the quartz crucible. Then, the quartz crucible, including the master alloys, was mounted in the chamber surrounded by spiral springs inside the glass-covered chamber. The distance between the wheel and the nozzle was adjusted to be 0.2 mm and the lid of the chamber was closed. Before pouring the melt on the disc, after the chamber containing the disc and crucible was vacuumed up to about 4×10^{-2} bar, the chamber was filled with argon gas and the disc velocity was set to 25 m/s. The master alloys were then melted and sprayed onto the copper disc with a pressure of about 300 mbar and ribbon alloys were obtained. As-received melt-spun ribbons were 6–10 mm in width and 40–60 μ m in thickness.

The crystallization behaviors and the corresponding dynamics of the as-received Ti-12V-4Al (wt. %) and Ti-12V-4Al-0.5Zr (wt. %) melt-spun ribbons were examined by differential scanning calorimetry (Setaram, DSC 131) with the different heating and cooling rate in the temperature range of 50–530 °C. The crystallization state and phase constituents were identified by the X-ray diffraction (Pixel3D) using $\text{CuK}\alpha$ radiation. Microstructures of ribbon samples were observed on optical microscope (Simadzu DUH-W201S). Samples for OM

observation were prepared by etching with a mixed solution of 10 ml HF, 20 ml HNO₃ and 40 ml H₂O after mechanical grinding and polishing. The surfaces of the melt-spun ribbons were observed by means of a scanning electron microscope (Quanta 200 FEG). The microstructural characterizations were carried out by transmission electron microscopy (JEM100SX) operating at an accelerating voltage of 200 kV. The samples for TEM observation were prepared by twin-jet electro-polishing in an electrolyte of 6 % perchloric acid, 60 % methyl alcohol and 34 % n-butyl alcohol by volume at about -30°C.

3. RESULTS AND DISCUSSION

Figure 1 shows DSC curves of the Ti-12V-4Al (wt. %) and Ti-12V-4Al-0,5Zr (wt. %) melt-spun ribbons at the temperature range 50–530 °C. DSC curves of the at heating / cooling rates of 30 °C / min are displayed in Figure 1.

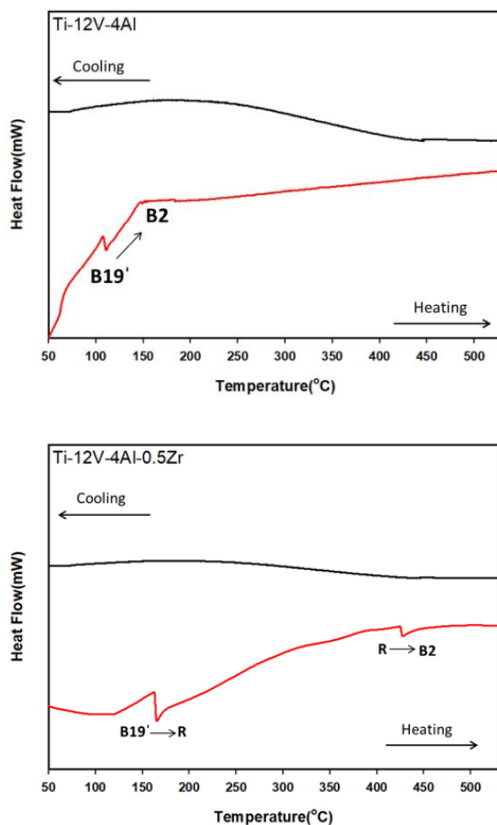


Figure 1 The DSC curves of Ti-12V-4Al (wt. %) and Ti-12V-4Al-0.5Zr (wt. %) melt-spun ribbons

In Figure 1, Ti-12V-4Al (wt. %) ribbon shows single-stage transformation. The martensite phase of the Ti-12V-4Al (wt. %) ribbon directly converts to austenite during heating (B19' martensite → B2 austenite). The endothermic peak is clearly visible at about 127 °C upon heating, which ends at 158 °C for Ti-12V-4Al (wt. %) ribbon. The DSC curve of Ti-12V-4Al-0.5Zr (wt. %) ribbon exhibits two endothermic peaks in heating, indicative of two-stage transformation (B19' martensite → R-phase → B2 austenite). Some Zr added alloys (such as Ti-Ni-Zr) [10] also show typical reversible phase transformation behavior of HTSMAs on heating or cooling, where the martensite phase transformation from B19' martensite to B2 austenite occurs in a two-stage process. The first stage is attributed to the B19' martensite → R-phase and the second stage is for the R-phase → B2 austenite transformation [11]. Furthermore, the high cooling rate leads to high solid solubility and grain orientation preference in the suction-cast alloy during rapid solidification. It is believed that the Zr addition on quaternary HTSMAs results in the change of structural features and lattice distortion during martensitic transformation, which has an important role to play in terms of controlling the transformation temperature and phase transition behavior during the temperature change [12]. Its origin cannot be identified by DSC alone. To explain the phenomena mentioned above, in situ XRD was applied to Ti-12V-4Al (wt. %) and Ti-12V-4Al-0.5Zr (wt. %) ribbons at room temperature, and the results are shown in Figure 2.

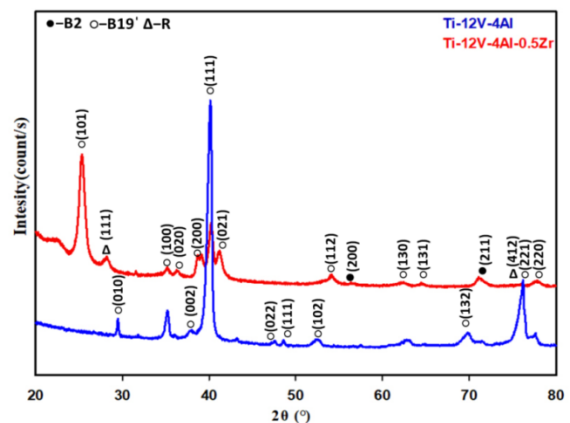


Figure 2 The XRD pattern of Ti-12V-4Al (wt. %) and Ti-12V-4Al-0.5Zr (wt. %) melt-spun ribbons

The Ti-12V-4Al (wt. %) and Ti-12V-4Al-0.5Zr (wt. %) ribbons are mainly at martensite state with B19' structure. The Ti-12V-4Al (wt. %) ribbon has a martensite phase indexed by (111) with a very strong peak at 39.89 degree and the Ti-12V-4Al-0.5Zr (wt. %) sample has a martensite phase indexed by (101) at 26.18 degree. In Ti-12V-4Al-0.5Zr (wt. %) ribbon, it can be seen that the intensity of B2 austenite peaks at diffraction angle of 56.12 and 73.56 degrees become. As seen in the graphic, R phases appeared at 27.84 and 46.34 degrees in the Ti-12V-4Al-0.5Zr (wt. %) ribbon. This is compatible with the phase transformations occurring in the DSC analysis and helps explain.

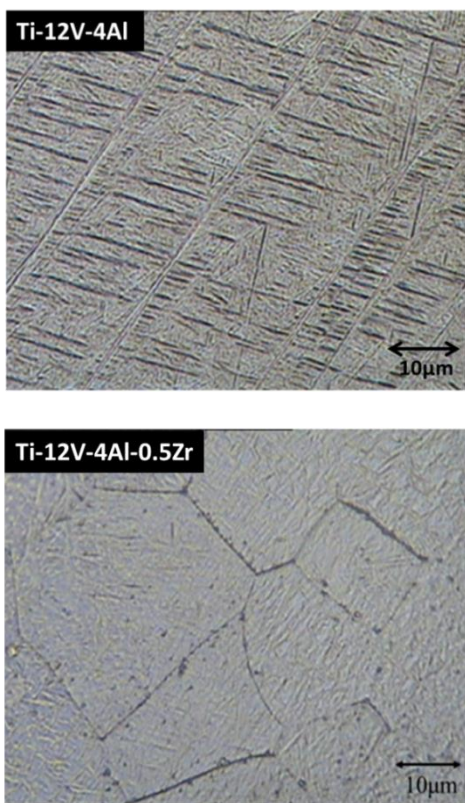


Figure 3 Optical images of Ti-12V-4Al (wt. %) and Ti-12V-4Al-0.5Zr (wt. %) melt-spun ribbons

Figure 3 shows the typical optical morphologies of the Ti-12V-4Al and Ti-12V-4Al-0.5Zr ribbons. Although Ti-12V-4Al ribbon is more pronounced in both samples, typical lath-shaped or thin acicular martensite phases are seen. The orientations of these martensite phases formed in the Ti-12V-4Al-0.5Zr ribbon differ in each grain. Compared to the Ti-12V-4Al ribbon produced, these phases are stacked finer, softer and more dispersed in the Ti-12V-4Al-0.5Zr ribbon. In

addition, it is seen that the grain boundaries of Ti-12V-4Al-0.5Zr ribbon emerge more clearly.

Figure 4 shows the SEM images taken at 10000 magnification of the ribbons. It is seen that the microstructures of the ribbons consist dominant martensite phases. A small amount of austenite phases are seen in the Ti-12V-4Al-0.5Zr (wt. %) ribbon. It is estimated that Zr element accumulates in grain boundaries in Ti-12V-4Al-0.5Zr (wt. %) ribbon. The XRD result of Ti-12V-4Al (wt. %) ribbon reveals only B19' martensite phase and no additional peak corresponding to was observed. In addition, in Ti-12V-4Al-0.5Zr (wt. %) ribbon, B2 phase is clearly seen and these results are considered to be compatible with XRD analysis.

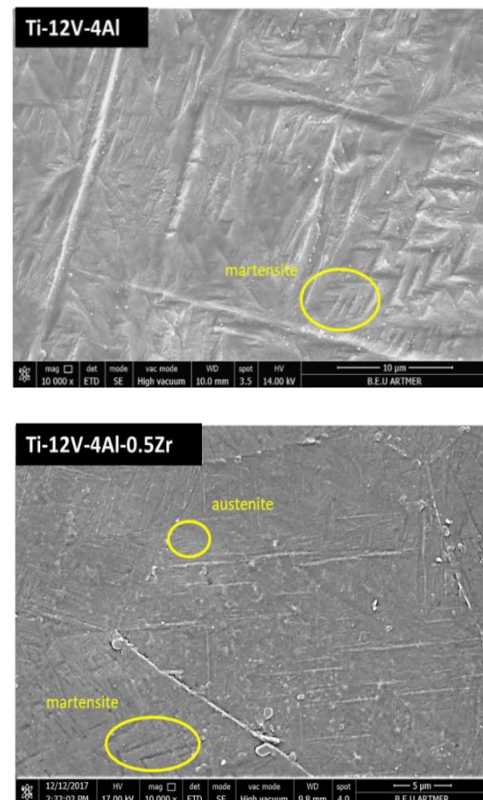
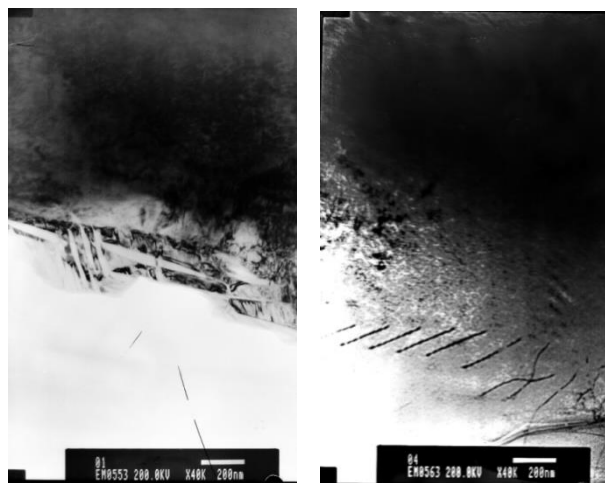


Figure 4 SEM images of the Ti-12V-4Al (wt. %) and Ti-12V-4Al-0.5Zr (wt. %) melt-spun ribbons

TEM images of melt-spun ribbons are depicted in Figure 5. The microstructure is featured with the parallel martensite plates with the width of 100-300 nm in Figure 5a. And various martensite variants distribute in mutually intersecting directions. In Figure 5b, the thickness of the martensite plates is slimmed and become obscure

with Zr amount in the ribbon, which can be ascribed to a decrease in the grain size [13, 14].



(a) Ti-12V-4Al (b) Ti-12V-4Al-0.5Zr

Figure 5 TEM images for (a) Ti-12V-4Al (wt. %) and (b) Ti-12V-4Al-0.5Zr (wt. %) melt-spun ribbons

4. CONCLUSION

In this research, we have examined the effects of Zr addition on the microstructure and shape memory properties Ti-12V-4Al and Ti-12V-4Al-0.5Zr melt-spun ribbons. The obtained results were as follows:

DSC results show that there is a two-stage B19' martensite \rightarrow R-phase \rightarrow B2 austenite transformation in Ti-12V-4Al-0.5Zr ribbon, while a single-stage B19' martensite \rightarrow B2 austenite transformation occurred in the Ti-12V-4Al ribbon.

In the optical microscope results, it was observed that the microstructure of the melt-spun ribbons contained martensite structures with a lath-shape, grain boundaries were clearly observed in the Ti-12V-4Al-0.5Zr ribbon.

SEM and XRD analyses confirmed that while the Ti-12V-4Al-0.5Zr ribbon consisted of B19' martensite B2 austenite and R phases, the Ti-12V-4Al was composed solely of a B19' martensite phase.

It was found from TEM observations that the size of martensite plates decreased with an increasing Zr amount.

Acknowledgements

The authors would like to thank the Gaziosmanpaşa University Scientific Research Projects Unit (BAP) for contributing to the financial portion of the project.

Funding

This project studies were supported by Gaziosmanpaşa University Scientific Research Projects Unit. Project numbers were 2017 / 95.

The Declaration of Conflict of Interest/ Common Interest

No conflict of interest or common interest has been declared by the authors.

Authors' Contribution

This study is the doctoral thesis of ÖZNUR BAĞ and the supervisor is UĞUR KÖLEMEN. UĞUR KÖLEMEN had a great contribution in providing support for the study, interpreting the findings. FİKRET YILMAZ contributed to resources, validation, device prototype and data analyses. SEMRA ERGEN helped to investigation, writing-review and visualization.

The Declaration of Ethics Committee Approval

The authors declare that this document does not require an ethics committee approval or any special permission.

The Declaration of Research and Publication Ethics

The authors of the paper declare that they comply with the scientific, ethical and quotation rules of SAUJS in all processes of the article and that they do not make any falsification on the data collected. In addition, they declare that Sakarya University Journal of Science and its editorial board have no responsibility for any ethical violations that may be encountered, and that this study has not been evaluated in any academic publication environment other than Sakarya University Journal of Science.

REFERENCES

- [1] C. M. Wayman, K. Otsuka, "Shape Memory Materials," Cambridge University Press, 1998.
- [2] R. D. Noebe, T. Biles, S. A. Padula, "NiTi-based high temperature shape-memory alloys: properties, prospects, and potential applications, in 'Advanced structural materials: properties, design optimization, and applications,' (ed. W. O. Soboyejo and T. S. Srivatsan); New York, Taylor & Francis Group, 2007.
- [3] Q. Li, J. Li, G. Ma, X. Liu, D. Pana, "Influence of ω phase precipitation on mechanical performance and corrosion resistance of Ti-Nb-Zr alloy," *Material and Design*, 11C, pp. 421-428, 2016.
- [4] J. Wang, Q. Li, C. Xiong, Y. Li, B. Sun, "Effect of Zr on the martensitic transformation and the shape memory effect in Ti-Zr-Nb-Ta high-temperature shape memory alloys," *Journal of Alloys and Compounds*, 737, pp. 672-677, 2018.
- [5] X. Yi, Y. Wang, B. Sun, B. Cui, J. Liu, X. Meng, Z. Gao, W. Cai, L. Zhao, "Crystallization process and microstructural evolution of as-spun Ti-Ni-Zr alloy ribbon," *Journal of Alloys and Compounds*, 762, pp. 62-66, 2018.
- [6] C. Xiong, L. Yaoa, B. Yuan, W. Qu., Y. Li, "Strain induced martensite stabilization and shape memory effect of Ti-20Zr-10Nb-4Ta alloy," *Materials Science&Engineering A*, 658, pp. 28-32, 2016.
- [7] O. Uzun, T. Karaaslan, M. Keskin, "Production and structure of rapidly solidified Al-Si alloys," *Turk J. Phys.*, 25:455-66, 2001.
- [8] O. Uzun, T. Karaaslan, M. Göğebakan, M. Keskin, "Hardness and microstructural characteristics of rapidly solidified Al-8-16 wt. % Si Alloys," *J. Alloys Compd.*, 376:149-57, 2004.
- [9] Y. Kim, Y. Yun, T. Nam, "The effect of the melt spinning processing parameters on the solidification structures in Ti-30 at.% Ni-20 at.% Cu shape memory alloys," *Mater Sci Eng A.*, 438-440:545-8, 2006.
- [10] H.Y. Kim, M. Mizutani, S. Miyazaki, "Crystallization process and shape memory properties of TieNieZr thin films," *Acta Mater.*, 57, 1920-1930, 2009.
- [11] Y. Motemani, P. J. McCluskey, C. W. Zhao, M. J. Tan, "Analysis of Ti-Ni- Hf shape memory alloys by combinatorial nanocalorimetry," *Acta Mater.* 59, 7602-7614, 2011.
- [12] Y. Y. Li, S. S. Cao, X. Ma, C. B. Ke, X. P. Zhang, "Influence of strongly textured microstructure on the all-round shape memory effect of rapidly solidified Ni51Ti49 alloy," *Materials Science & Engineering A.*, 705, 273-281, 2017.
- [13] S. Ergen, O. Uzun, F. Yılmaz, F. Kiliçaslan, "Shape memory properties and microstructural evolution of rapidly solidified CuAlBe alloys," *Materials Characterization*, 80, pp. 92-97, 2013.
- [14] Ö. Bağ, F. Yılmaz, U. Kölemen, S. Ergen, C. Temiz and O. Uzun, "Transformational, microstructural and superelasticity characteristics of Ti-V-Al high temperature shape memory alloys with Zr addition," *Physica Scripta*, Vol. 96, 8, 2021.